Vol. 19, No. 3 (2020) 1175-1185
Revista Mexicana de Ingeniería Química

Detection of *Salmonella enterica* on silicon substrates biofunctionalized with anti-*Salmonella* IgG, analyzed by FTIR spectroscopy

Detección de *Salmonella enterica* sobre sustratos de silicio biofuncionalizados con IgG anti-*Salmonella*, analizados por espectroscopía FTIR

F.J. Gómez-Montaño[1], A. Orduña-Díaz[1*], M.C.G. Avelino-Flores[2], F. Avelino-Flores[2], F. Ramos-Collazo[2], C. Reyes-Betanzo[3], V. López-Gayou[1]

[1]*Centro de Investigación en Biotecnología Aplicada del Instituto Politécnico Nacional. Ex Hacienda San Juan Molino Carretera Estatal Tecuexcomac-Tepetitla Km 1.5. C.P. 90700. Tlaxcala, México.*
[2]*Benemérita Universidad Autónoma de Puebla. Avenida San Claudio s/n, Ciudad Universitaria, La Hacienda. C.P. 72592. Puebla, Puebla, México.*
[3]*Instituto Nacional de Astrofísica, Óptica y Electrónica. Luis Enrique Erro #1, Santa María Tonanzintla. C.P. 72840. San Andrés Cholula, Puebla, México.*

Received: November 13, 2019; Accepted: January 11, 2020

Abstract

Salmonella enterica was detected at a concentration of 500 CFU/mL. For this, three substrates were used (crystalline and amorphous silicon, hydrogenated amorphous silicon carbide) with an area of 25 mm^2, functionalized by the self-assembled monolayers (SAM) technique. Characteristic functional groups of SAMs were observed (-NH_2, -C=O, Si-O-Si, Amide I, Amide II) by the Fourier transform infrared spectroscopy (FTIR) technique. Anti-*Salmonella* IgG antibodies were generated. To determine the secondary structure of proteins, second derivative of each FTIR detection spectrum was generated, observing modifications in the zone between 1600-1700 cm^{-1}, which corresponds to the region of proteins, specifically to structures of β-sheets and β-turns, as a result, substrates or platforms of crystalline silicon and hydrogenated amorphous silicon carbide showed band frequencies with higher intensity, being this attributed to a better sensitivity, which are proposed for applications in the development of biosensors for the monitoring of microbial quality in foods.

Keywords: biosensor, silicon, FTIR, Salmonella, IgG.

Resumen

Se realizó la detección de *Salmonella enterica* a una concentración de 500 UFC/mL. Para esto se emplearon tres sustratos (silicio cristalino y amorfo, carburo de silicio amorfo hidrogenado) con un área de 25 mm^2, funcionalizados mediante la técnica de autoensamble en monocapas (SAMs). Se observaron los grupos funcionales característicos del ensamble (-NH_2, -C=O, Si-O-Si, Amida I, Amida II) por la técnica de espectroscopia infrarroja por transformada de Fourier (FTIR). Se generaron anticuerpos IgG anti-*Salmonella*. Para determinar la estructura secundaria de las proteínas, se generó la segunda derivada de cada espectro FTIR de detección, observando modificaciones en la zona de 1600-1700 cm^{-1}, que corresponde a la región de las proteínas, específicamente estructuras de hojas y giros β, obteniendo como resultado que los sustratos o plataformas de silicio cristalino y carburo de silicio amorfo hidrogenado mostraron bandas con mayor intensidad, atribuyéndose a una mejor sensibilidad, los cuales se proponen para aplicaciones en el desarrollo de biosensores para el monitoreo de la calidad microbiana en alimentos.

Palabras clave: biosensor, silicio, FTIR, Salmonella, IgG.

1 Introduction

Foodborne illness is an important public health problem with major economic and social effects, in terms of morbidity and mortality; they have enormous implications for primary industry, food manufacturing and retail industry and also for trading (Odeyemi, 2016). Many outbreaks and individual cases of foodborne illness are caused from consuming the two most common types of foodborne pathogens: bacteria (*Salmonella, Escherichia coli* or *Listeria*) and viruses (norovirus, hepatitis A) (FDA, 2018).

* *Corresponding author. E-mail*: abdueve@hotmail.com
https://doi.org/10.24275/rmiq/Bio993
issn-e: 2395-8472

In Latin America and other regions, *Salmonella* is considered one of the most common causes of foodborne diarrheic outbreaks (Fuzihara *et al*., 2000), being *Salmonella* enteriditis and *Salmonella* typhimurium the most important serotypes transmitted from animals to humans, which induce gastrointestinal diseases that may be dangerous in children, elderly and immunocompromised patients (WHO, 2018), because of this, detection and identification of bacterial pathogens (specially *Salmonella*) remain a high priority goal, considering that conventional culture-based assays are inherently time consuming and labor intensive (Burlage *et al*., 2017), bacteria detection is moving to methods more rapid, sensitive, precise, and low-cost (Zhang *et al*., 2017). Thus, successful pathogen-diagnostic and detection systems that overcome the aforementioned need to be developed (Yoo *et al*., 2016); Biosensors might be an option for rapid and sensible determination, by definition a biosensor is an analytical device that integrates a biological recognition element derived from molecules such as enzymes, antibodies, phages, aptamers, or single-stranded DNA join a suitable physicochemical transducer (Bahadir *et al*., 2015).

Through the development of biosensor technology, these devices have received significant attention as tools in analytical and diagnostics applications (Crivianu-Gaita *et al*., 2016) in areas such as medical field, environment, agriculture and biological safety (Sharma *et al*., 2019); interest in biosensors extends not only to research but also to industry where detection, diagnosis and determination of biomolecules are high priorities (Lepinay *et al*., 2014), fabrication of this kind of dispositives, its materials, transducing mechanism and immovilization methods requires multidisciplinary research in chemistry, biology, and engineering (Mehrotra, 2016).

Novel materials or fabrication process, using for example transparent glass or silicon substrates as platforms to develop biosensors, could be a competitive alternative in a near future to improve integration and miniaturization, but silicon is still the workhorse of the IO photonic research and industry (Fernández *et al*., 2016). Silicon is the eighth most abundant element in the solar system (Lutgens *et al*., 2000) and it is the material of choice for Micro-Electro Mechanical Systems (MEMS) applications (Joseph *et al*., 2017), some derivatives from silicon can be obtained like: amorphous silicon (aSi), which can be deposited on large areas and at low temperatures (Dahmen *et al*., 2003) in the form of thin films of low cost and mass production (Budini *et al*., 2007), hydrogenated amorphous silicon carbide (aSiCH), another derivative from silicon, is chemically stable, it reduces the dissolution of the material when it is placed into a wet solution (Saddow, 2012) and it has been used in some biosensor applications (Knaack *et al*., 2016); one of the techniques used to functionalized and biofunctionalized silicon based material is known as Self-Assembly Monolayers (SAMs) that is the coordinated action of independent molecular/atomic species distributed under control to produce organized structures or superstructures with certain specific patterns (Aslam *et al*., 2003).

Based on the aforementioned, the objective of this work was to develop and standardized a methodology that allow us to detect *Salmonella enterica* by using three different silicon substrates and its derivatives biofunctionalized with an immunoglobulin G (IgG) against Salmonella, each part of SAMs technique was analyzed by Infrared Spectroscopy Fourier Transform (FTIR) obtaining second derivate from each FTIR biofunctionalization and detection spectra.

2 Materials and methods

2.1 Obtaining, purification and characterization of an IgG anti-Salmonella polyclonal antibody

Attenuated bacteria of *Salmonella* typhimurium ATCC 14028 (Instituto de Ciencias Microbiológicas from Benemérita Universidad Autónoma de Puebla) was employed as antigen, polyclonal anti-*Salmonella* antibody was obtained by immunizing a rabbit New Zealand (*Oryctolagus cuniculus*) (Bioterio Claude Bernard from Benemérita Universidad Autónoma de Puebla) intramuscularly with the antigen prepared, Freund's complete adjuvant (Sigma Aldrich) was used at the first immunization (Day 0), subsequent immunizations were performed with incomplete Freund's adjuvant (Sigma) (Days 21, 31 and 38). Blood samples were taken from the main vein of the rabbit's ear. Blood was collected in a test tube without anticoagulant to be centrifuged for 10 min at 3500 rpm at 25 ºC. The production of polyclonal antibodies was tested by a Dot-ELISA assay of the sera samples obtained on days 0, 21, 31 and 38, according to the modified method proposed by Cervantes-Landín et al (2014).

After confirming the presence of IgG anti-*Salmonella*, the blood was extracted from the rabbit

by cardiac puncture to proceed with obtaining the serum and subsequent purification of antibodies using a Protein A IgG purification kit (Thermo Fischer Scientific). IgG concentration was determined by Bradford method (Bradford, 1976) and it was characterized by FTIR (FT-IR Bruker Vertex 70) with diamond attenuated total reflection (ATR) in the range of 4000-400 cm^{-1} using air as base line, data were recorded at room temperature, 120 scans were taken with a resolution of 4 cm^{-1} from each sample. Second derivative of antibody spectrum was obtained using OriginLab 6.0 Software.

2.2 SAMs process on each silicon-based material substrates

Substrates used were p-type commercial silicon crystalline (100, Pure Wafer) and aSiCH and aSi films were synthesized at Instituto Nacional de Astrofísica, Óptica y Electrónica (INAOE) by PECVD method; substrates were cut into 5x5 mm pieces.

Ultrasonic cleaning process was performed by immersion of each substrate in acetone (Meyer) and in methanol (Meyer), after this, nitrogen flow was used in order to eliminate humidity on the materials and finally they were collocated into a convection oven (lumistell IEC-41) at 110 ºC during 30 min.

To obtain hydroxyl groups on the surfaces, the films were treated with H_2SO_4:H_2O_2 (3:1) for 30 min (H_2SO_4 and H_2O_2 are both from Meyer), after this process, substrates were ultrasonic cleaned three times with deionized water, drying was carried out with N_2 flow and then put in an oven at 110 ºC during 30 min. In order to generate amino groups on the surfaces, a solution 2% of (3-aminopropyl) trimethoxy silane (3-APTMS, Sigma Aldrich) in anhydrous toluene from Sigma Aldrich (previously heated to 100 ºC and cooled down to 25 ºC), all substrates were immersed in 3-APTMS solution for 1 h, then ultrasonic cleaned was carried out by using toluene and methanol, drying was realized in an oven at 110 ºC during 1 h. a 2.5% solution of Glutaraldehyde (GA, Sigma Aldrich) in PBS (pH 7.4) was used as crosslinker, then each film was put into the solution for 1 h at 25 ºC/300 rpm, after this substrates were cleaned with 200 μL of MilliQ water.

The antibody generated in previous steps was used as biological recognition element; platforms were immersed in a solution of antibody (0.01 mg/mL) in PBS (pH 7.4) during 1 h at 4 ºC, cleaning was made three times with 200 μL of PBS during 5 min each one and finally the substrates were stored in 500 μL of PBS at 4 ºC. After finishing each of the self-assembly monolayer stages, substrates were analyzed by FTIR.

2.3 Detection of Salmonella typhimurium on each substrate and subsequent characterization by FTIR technique

For the detection process, each biofunctionalized substrate was placed in 400 μL of bacterial suspension (500 CFU/mL approximately), then it was incubated for 1 h at 37 ºC, after this 3 washes were made to each substrate with 200 μL of PBS and subsequent was analyzed by FTIR, to proceed with the calculation of the second derivative of the different spectra obtained (detection process and bacteria) by using OriginLab 6.0 Software.

3 Results and discussion

3.1 Obtaining, purification and characterization of an IgG anti-Salmonella polyclonal antibody

Sera samples from the rabbit immunized were subjected to a Dot-ELISA test. Figure 1 shows dots resultant, positive result was considered in dots with dark coloration, while the negative sample showed a faint signal. According to this, control sample as well as the sample from day 0 were negative in comparison to the days 21, 31, 38 which high intensity is related to the number of immunizations performed to the host since the vaccination schemes with long periods and repeated reinforcements increase the development of antibodies against the inoculated antigen (Vogel *et al*., 1995).

Once confirmed the presence of antibodies, the host was sacrificed on day 45, 10 vials of purified antibody were obtained, concentrations of IgG proteins by Brandford method were determined between 0.9-2.5 mg/mL. According to the user manual of the purification column, the highest amount of IgG is in the first tubes of antibody elution and this decreases as the process continues.

Polypeptides and proteins give rise to nine characteristic IR absorption bands, where amide I and amide II are the two most prominent proteins bands (Surewicz *et al*., 1988), in figure 3 purified IgG antibody FTIR spectrum is observed, where band between 1700-1600 cm^{-1} corresponds almost entirely to the stretching vibration modes of C=O from peptide

bonds, while amide II signals are between 1550 - 1600 cm^{-1} derived from in-plane N-H bending and from C-N stretching vibration (Kong *et al*., 2007), it is observed that the band corresponding to amide I is more intense that the band related to amide II, likewise C-S stretching vibration modes (692 cm^{-1}), CH_2-CH-SH bending vibration modes (444 cm^{-1}) and bending modes in the plane from the S-H bond (1064 cm^{-1})(Parker, 2013). are related to disulfide bridges bonds, as well as cysteine and methionine amino acids (Smith *et al*., 1955).

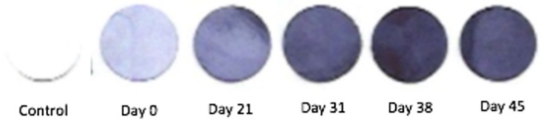

Fig. 1. Results of Dot ELISA test from blood serum samples at different days of immunization.

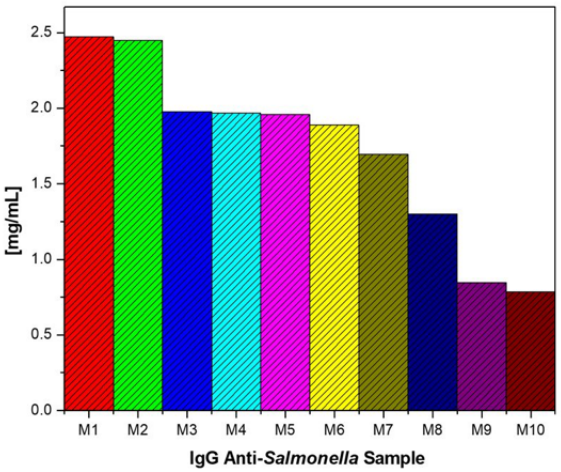

Fig. 2. Concentrations of purified IgG antibody (mg/mL) determined in 10 samples.

3.2 *SAMs process on each silicon-based material substrates*

Structural properties and presence of characteristic functional groups of the molecules and biomolecules used in the development of SAMs were studied by FTIR technique in middle infrared (400-4000 cm^{-1}).

Functional groups as carbonyl or amine can interact with the functionalities of the inorganic phase (Castruita-de León *et al*., 2018). In Figure 4 and 5, spectra of functionalization with 3-APTMS and GTA on cSi and aSi are observed, comparing both materials similar spectra were obtained, this because FTIR technique is used to confirm the presence of functional groups but it does not indicate structure of the material; unlike aSiCH (Figure 6) where a different spectrum was gotten; in all cases, it can be observed in untreated substrates spectra bands related to Si-O stretching vibration modes at 616 cm^{-1} and 1100 cm^{-1} (bond generated by the interaction of the substrate surface with oxygen present in the environment, previous activation), Si-H (640 cm^{-1} wagging mode and 2000 cm^{-1} stretching vibration modes), $Si-H_2$ (2090 cm^{-1} stretching vibrational modes); specifically bands related to Si-C bonds (750-780 cm^{-1}) in stretching mode were observed in aSiCH (Herrera-Celis *et al*., 2015). For the functionalization process with 3-APTMS, silanes are bound through the formation of a Si-O-Si bond between treated surface and silanol groups (Yamaura *et al*., 2004; Taylor *et al*., 2000; Liu *et al*., 2005). Comparing spectra, it is observed the appearance of bands related to Si-O-Si in 1035 and 1150 cm^{-1}, for scissoring and asymmetric stretching mode respectively (Majoul *et al*., 2015), presence of amino groups (-NH_2) is revealed with bands in wavenumber with value of 1570 cm^{-1} (scissoring vibration mode).

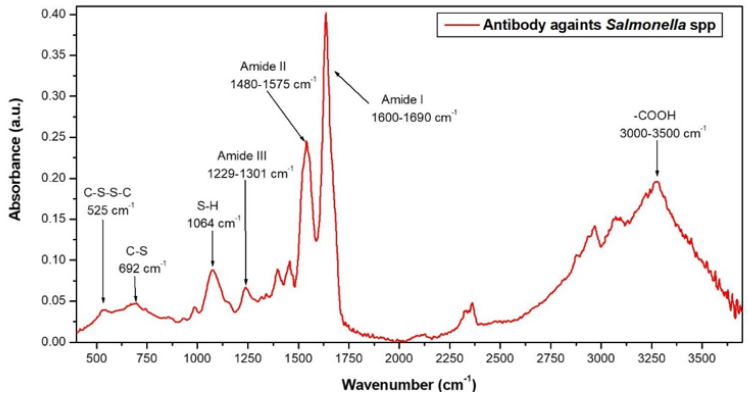

Fig. 3. Infrared spectrum of purified IgG, analyzed in ATR mode.

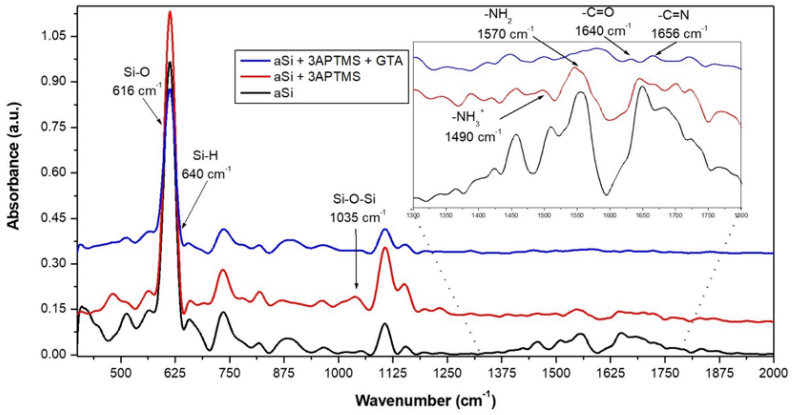

Fig. 4. IR spectra of GTA functionalization on amorphous silicon substrates, analyzed in transmission mode.

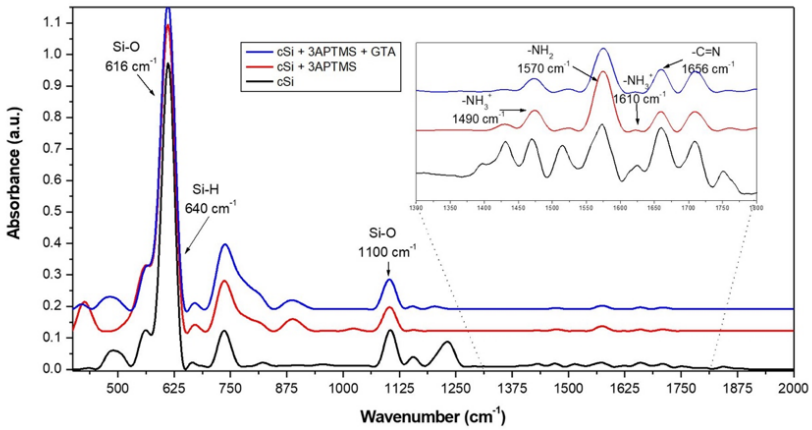

Fig. 5. IR spectra of GTA functionalization on crystalline silicon substrates, analyzed in transmission mode.

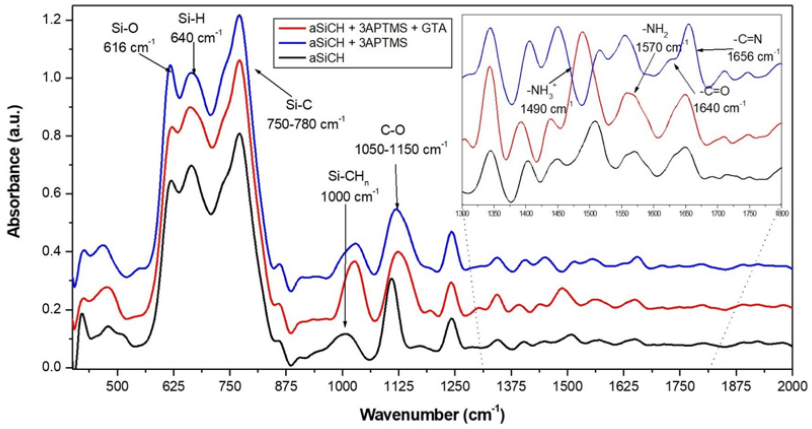

Fig. 6. IR spectra of GTA functionalization on hydrogenated amorphous silicon carbide substrates, analyzed in transmission mode.

In addition, we have a band of low intensity at 1490 cm^{-1} assigned to the symmetric deformation mode of NH_3^+, presence of this vibration mode suggests that when samples are exposed to air humidity, water molecules are weakly adhered to the amino groups, which allows the protonation of this functional group (González-Calderón *et al*., 2018; Mondal, 2018; Pasternack *et al*., 2008).

Finally, GA was used to activate substrates terminated in amine functional groups, through a terminal carbonyl group to form an imine, imine can even become an amide (Ducker *et al*., 2008).

Saini et al in 1993 reported the generation of bands corresponding to the vibrations of -C=O assigned to the band located at 1740 cm^{-1}, C=N stretching vibration modes (1649-1664 cm^{-1}) as well as the C-N bond (1395 cm^{-1}) of the amide, first two vibrational bands were observed in this work (Figure 4, 5 and 6).

After performing biofunctionalization of the different substrates with the obtained antibodies, we proceeded with their respective analysis by using FTIR, the zone between 1400-1800 cm^{-1} was analyzed, this area is assigned to the vibrations of molecular bonds present in proteins. It is reported that proteins have been immobilized on silica surfaces by covalent bond formation between functional groups of proteins (e.g. NH_2) and complementary groups (e.g. aldehyde or epoxides) (Zheng *et al*., 2005), so it is expected that the interaction occurring in the biofunctionalization carried out in this project was through this kind of interaction such as the one described by Batalla et al in 2009, in Figure 7 and 8, presence of amide I and amide II bands is observed in both spectra while for aSiCH (Figure 9), these bands are not very noticeable, but comparing with the lower spectrum (aSiCH+APTMS+GTA) an increase in the intensity of these bands is observed.

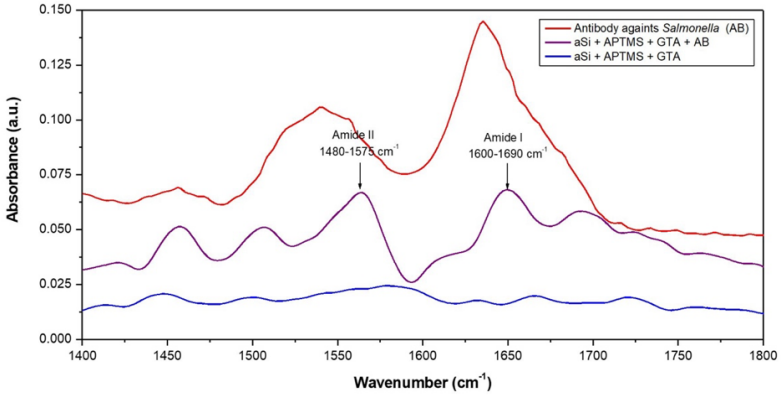

Fig. 7. Biofunctionalization IR spectra on amorphous silicon substrates, analyzed in transmission mode.

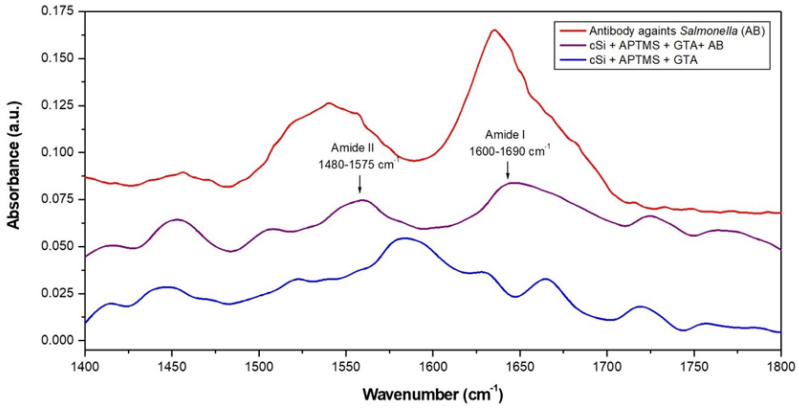

Fig. 8. Biofunctionalization IR spectra on crystalline silicon substrates, analyzed in transmission mode.

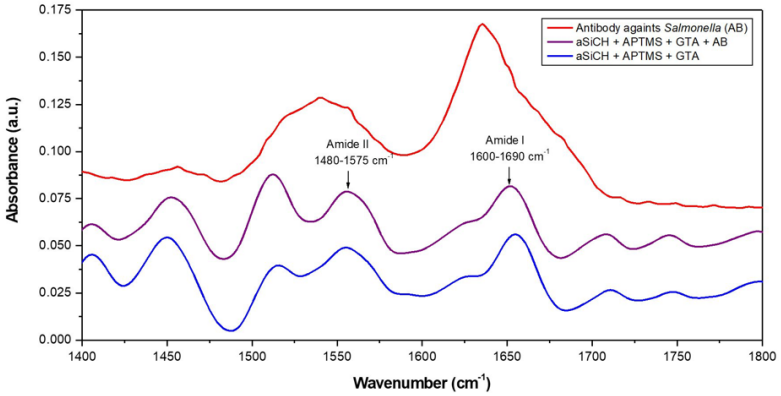

Fig. 9. Biofunctionalization IR spectra on hydrogenated amorphous silicon carbide substrates, analyzed in transmission mode.

3.3 Detection of Salmonella typhimurium on each substrate and subsequent characterization by FTIR technique

Antigen-antibody reaction, occurs from the contact between an antigen with an antibody (Cabrera, 2011); contact and bonding will depend upon the adaptation stability, this interaction can be modified by external factors such as temperature, pH, ionic strength, time of incubation, antigen concentration and antigen-antibody structure (Vargas *et al*., 2014).

Spectra of biofunctionalized substrates with detection process were used in order to calculate second derivative of each of them, in order to analyze the secondary structure of proteins, in this case of proteins present in bacteria of interest (~ 3,300 bacterial proteins identified in *Salmonella* typhimurium strain; Liu *et al*., 2015). To carry out this step, we utilized the analysis of amide I (1700-1600 cm^{-1}), since it is reported that the high sensitivity to small variations in molecular geometry and hydrogen bonding patterns and the vibration of this group that is reflected to the secondary structure (Dong *et al*., 1990) makes it possible to study the folding, unfolding and aggregation of proteins with infrared spectroscopy (Barth, 2007). In figure 10, calculated second derivatives for the spectra corresponding to biofunctionalization and detection are shown, at the top *Salmonella* typhimurium ATCC 14028 second derivative was collocated, in the three spectra of each substrate the band at 1642 cm^{-1} is observed and it is related to β-sheets structure (Kong *et al*., 2007; Barth, 2007 & Natalello *et al*., 2005) this band is present in antibody and bacteria spectra as well, it also can be highlighted the presence of two bands, one in 1675 cm^{-1} and one in 1690 cm^{-1} (β-turns and β-sheets, respectively) (Kong *et al*., 2007; Barth, 2007 & Natalello *et al*., 2005) which are not present in the biofunctionalized substrates and that can be used to confirm the detection of the bacteria on each one of the substrates.

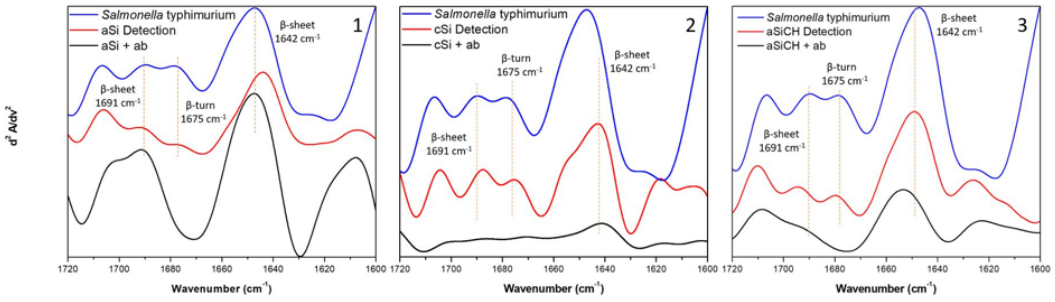

Fig. 10. Second derivative spectra obtained from each detection (1) aSi, (2) cSi and (3) aSiCH. Where it is shown from bottom to top: biofunctionalization, detection of bacteria and *Salmonella* typhimurium sample.

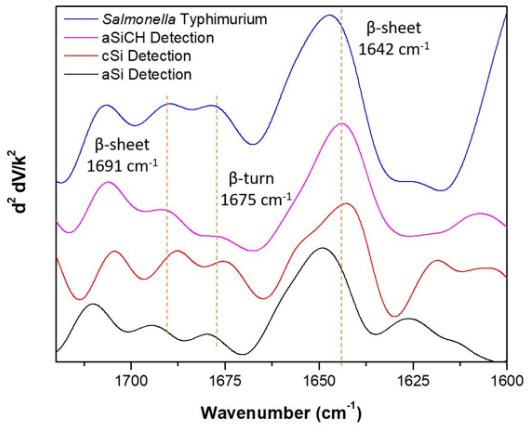

Fig. 11. Comparison of different detection second derivative spectra with *Salmonella* typhimurium second derivative spectrum.

In comparison with other studies where *Salmonella* typhimurium has been detected (Alexandre *et al*., 2018; Yang *et al*., 2009), detection was performed on flat substrates with a specific area (25 mm^2) and a detection time of 60 min was stablished, in addition a concentration of 500 CFU/mL was detected in comparison with Seo et al (1999) who detected between $1\times10^5 - 1\times10^7$ CFU/mL in a silane-derived sensor surface. In Figure 11 a comparison of each detection process with the second derivative FTIR spectrum of Salmonella is made, in which it can be seen that bands are more defined in cSi and aSiCH spectra than in aSi spectrum, with this study these materials have an opportunity for being used in the development of biosensors.

Conclusions

Detection of *Salmonella enterica* was successful due to the optical and chemical properties of the three substrates in conjunction with the specificity given by the generated antibodies, a fundamental characteristic of the biological recognition element, thus facilitating the interaction with the bacterium aforementioned. Second derivative spectra showed on cSi and aSiCH biosensors more intense bands in comparison with aSi biosensor; with the analysis made on detection process, it was observed that bands between 1675-1690 cm^{-1} can be used for a specific *Salmonella* detection by using FTIR. Results suggest the use of these biosensors in future applications to detect this pathogen microorganism in food and clinical areas.

Acknowledgements

The first author thanks the support to Consejo Nacional de Ciencia y Tecnología (CONACYT) for the scholarship granted to study the Doctorate in Biotechnology Sciences within the doctorate program of the Instituto Politécnico Nacional, included in the list of Postgraduate Degrees of Excellence.

References

Alexandre, D.L., Melo, A.M.A., Furtado, R.F., Borges, M.F., Figueiredo, E.A.T., Biswas, A., Cheng, H.N. & Alves, C.R. (2018). A rapid and specific biosensor for *Salmonella* typhimurium detection in milk. *Food and Bioprocess Technology 11*, 748-756.

Aslam, M., Chaki, N.K., Sharma, J. & Vijayamohanan, K. (2003). Device applications of self-assembled monolayers and monolayer-protected nanoclusters. *Current Applied Physics 3*, 115-127.

Barth, A. (2007). Infrared spectroscopy of proteins. *Biochimica et Biophysica Acta 1767*, 1073-1101.

Batalla, P., Mateo, C., Grazu, V., Fernandez-Lafuente, R. & Guisan, J.M. (2009). Immobilization of antibodies through the surface regions having the highest density in lysine groups on finally inert support surfaces. *Process Biochemistry 44*, 365-368.

Bradford, M.M. (1976). A rapid and sensitive method for the quantitation of microgram quantities of protein utilizing the principle of protein-dye binding. *Analytical Biochemistry 7*, 248-254.

Budini, N., Schmidt, J.A., Arce, R. & Buitrago, R.H. (2007). Silicio amorfo hidrogenado como material para la obtención de láminas delgadas de silicio policristalino. *ANALES AFA 182*, 182-186.

Burlage, R.S. & Tillmann, J. (2017). Biosensors of bacterial cells. *Journal of Microbiological Methods 138*, 2-11.

Cabrera, M.J. (2011). *Serología de la Reacción Antígeno-Anticuerpo*. Fesitess. Andalucía, España.

Castruita-de León, G., Meléndez-Ortíz, H.I., Perera-Mercado, Y.A., Mercado-Silva, J.A., García-Cerda, L.A., Montes-Luna, A. de J. & García-Rodríguez, S.P. (2018). Effect of silica source on the synthesis and properties of polysulfone/silica composite membranes for gas separation. *Revista Mexicana de Ingeniería Química 17*, 693-705.

Cervantes-Landín, A.Y., Martínez-Martínez, I., A. Reyes., P., Shabib, M., Espinoza-Gutiérrez, B. (2014). Estandarización de la técnica Dot-ELISA para la detección de anticuerpos anti-*Trypanosoma cruzi* y su comparación con ELISA y Western blot. *Enfermedades Infecciosas y Microbiología Clínica 32*, 363-368.

Crivianu-Gaita, V. & Thompson, M. (2016). Aptamers, antibody scFv, and antibody Fab' fragments: An overview and comparison of three of the most versatile biosensor biorecognition elements. *Biosensors and Bioelectronics 85*, 32-45.

Dahmen, C., Janotta, A., Dimova-Malinovska, D., Marx, S., Jeschke, B., Nies, B., Kessler, H. & Stutzmann, M. (2003). Surface functionalization of amorphous silicon and silicon suboxides for biological applications. *Thin Solid Films 427*, 201-207.

Dong, A., Huang, P., Caughey, W.S. (1990). Protein secondary structure in water from second-derivative amide I infrared spectra. *Biochemistry 29*, 3303-3308.

Ducker, R.E., Montague, M.T. & Leggett, G.J. (2008). A comparative investigation of methods for protein immobilization on self-assembled monolayers using glutaraldehyde, carboniimide, and anhydride reagents. *Biointerphases 3*, 59-65.

Fernández-Gavela, A., Grajales-García, D., Ramírez, J.C. & Lechuga, L.M. (2016). Last advances in silicon-based optical biosensors. *Sensors 16*, 1-15.

Food and Drugs Administration (2018). Most common foodborne illnesses. Available in: https://www.fda.gov/files/food/published/Most-Common-Foodborne-Illnesses-%28PDF%29.pdf Access day: May 31, 2019.

Gonzalez-Calderon, J.A., Vallejo-Montesinos, J., Martínez-Martínez, H.N., Cerecero-Enríquez, R. & López-Zamora, L. (2019). Effect of chemical modification of titanium dioxide particles via silanization under properties of chitosan/potato-starch films. *Revista Mexicana de Ingeniería Química 18*, 913-927.

Herrera-Celis, J., Reyes-Betanzo, C., Itzmoyotl-Toxqui, A., Orduña-Díaz A. & Pérez-Coyotl, A. (2015). A.SixC1-x:H thin films with subnanometer surface roughness for biological applications. *Journal of Vacuum Science and Technology A 33*, 1-7.

Joseph, J., Govind Singh, S., Krishna Vanjari, S.R. (2017). Ultra-smooth e-beam evaporated amorphous silicon thin films- A viable alternative for PECVD amorphous silicon thin films for MEMS applications. *Material Letters 197*, 52-55.

Knaack, G.L., Charkhkar, S.F., Cogan, J.J., Pancrazio & Saddow, S.E. (2016). *Silicon Carbide Biotechnology*. 2nd Ed. Amsterdam, Elsevier. Ed. S.E. Saddow, 249.

Kong, J. & Yu S. (2007) Fourier transform infrared spectroscopic analysis of protein secondary structures. *Acta Biochimica et Biophysica Sinica 39*, 549-559.

Lepinay, S., Staff, A., Ianoul, A. & Albert, J. (2014). Improved detection limits of protein optical fiber biosensors coated with gold nanoparticles. *Biosensors and Bioelectronics 52*, 337-344.

Liu, Y., Zhang, Q., Hu, M., Yu, K., Fu, J., Zhou, F., Liu, X. (2015). Proteomic analyses of intracellular *Salmonella enterica* serovar typhimurium reveal extensive bacterial adaptations to infected host epithelial cells. *Infectimmun 83*, 2897-2906.

Liu, Z., Li, Z., Zhou, H., Wei, G., Song, Y. & Wang, L. (2005). Immobilization and condensation of DANN with 3-aminopropyltriethoxysilane studied by atomic force microscopy. *Journal of Microscopy 218*, 233-239.

Lutgens, F.K., Tarbuck, E.J. (2000). *Essentials of Geology*. 7th Ed. Upper Saddle River, NJ: Prentice Hall.

Majoul, N., Aouida, S. & Bessaïs, B. (2015). Progress of porous silicon APTES-functionalization by FTIR investigations. *Applied Surface Science 331*, 388-391.

Mehrotra, P. (2016). Biosensors and their applications-a review. *Journal of Oral Biology and Craniofacial Research 6*, 153-159.

Mondal, S. (2018). UNIT-II: Aromatic Amines: Basicity of amines, effect of substituents on basicity, and synthetic uses of aryl diazonium salts. Available in: https://www.researchgate.net/publication/326246546_UNIT-II_Aromatic_Amines_Basicity_of_amines_effect_of_substituents_on_basicity_and_synthetic_uses_of_aryl_diazonium_salts Access day: June 1, 2019.

Natalello, A., Ami, D., Brocca, S., Lotti, M. & M. Doglia, S. (2005). Secondary structure, conformational stability and glycosylation of a recombinant *Candida rugosa* lipase studied by Fourier-transform infrared spectroscopy. *Biochemical Journal 385*, 511-517.

Odeyemi, O.A. (2016). Public health implications of microbial food safety and foodborne diseases in developing countries. *Food & Nutrition Research 60*, 1-2.

Parker, S.F. (2013). Assignment of the vibrational spectrum of L-cysteine. *Chemical Physics 424*, 75-79.

Pasternack, R.M., Rivillion, S. & J. Chabal, Y. (2008). Attachment of 3-(aminopropyl)triethoxysilane on silicon oxide surfaces: dependence on solution temperature. *Langmuir 24*, 12963-12970.

Saddow, E. (2012). *Silicon Carbide Biotechnology: A Biocompatible Semiconductor for Advanced Biomedical Devices and Applications*, 1st Ed. Elsevier Science. Ed. S.E. Saddow, 17-61.

Saini, A.K., Carlin, C.M. & Patterson, H.H. (1993). Confirmation of the presence of imine bonds in thermally cured polymides. *Journal of Polymer Science: Part A, Polymer Chemistry 31*, 2751-2758.

Seo, K.H., Brackett, R.E., Hartman, N.F. & Campbell, D.P. (1999). Development of a rapid response biosensor for detection of *Salmonella* typhimurium. *Journal of Food Protection 62*, 431-437.

Sharma, A., Sharma, N., Kumari, A., Lee, H., Kim, T. & Tripathi, K.M. (2019). Nano-carbon based sensors for bacterial detection and discrimination in clinical diagnosis: A junction between material science and biology. *Applied Materials Today*. https://doi.org/10.1016/j.apmt.2019.100467.

Smith, E.L., McFadden, M.L., Stockell, A. & Buettner-Janusch, V. (1955). Amino acid composition of four rabbit antibodies. *Journal of Biological Chemistry 214*, 197-207.

Surewicz, W.K. & Mantsch, H.H. (1988). New insight into protein secondary structure from resolution-enhanced infrared spectra. *Biochimica et Biophysica Acta 952*, 115-130.

Taylor, A.P., Webb, R.I., Barry, J.C., Hosmer, H., Gould, R.J. & Wood B.J. (2000). *Journal of Microscopy 199*, 56-57.

Vargas, T. & Flores, T. (2014). Reacciones antígeno-anticuerpo. *Revista de Actualización Clínica 44*, 2319-2324.

Vogel, F.R., Powell, M.F. (1995). *A Summary Compendium of Vaccine Adjuvants and Excipients. Vaccine Design: The Subunit and Adjuvant Approach*. New York, USA. Plenum Publishing Corp. 234-250.

World Health Organization (2018). *Salmonella* (non-typhoidal). Available in: https://www.who.int/news-room/fact-sheets/detail/salmonella-(non-typhoidal) Access day: May 31, 2019.

Yamaura, M., Camilo, R.L., Macêdo, M.A. Nakamura, M. & Toma, H.E. (2004). Preparation and characterization of (3-aminopropyl) triethoxysilane-coated magnetite nanoparticles. *Journal of Magnetism and Magnetic Materials 279*, 210-217.

Yang, G.J., Huang, J.L., Meng, W.J., Shen, M. & Jiao, X.A. A reusable capacitive immunosensor for detection of *Salmonella* spp. Based on grafted ethylene diamine and self-assembled

gold nanoparticle monolayers. *Analytica Chimica Acta 647*, 159-166.

Yoo, S.M. & Lee, S.Y. (2016). Optical biosensors for the detection of pathogenic microorganisms. *Trends in Biotechnology 34*, 7-25.

Zhang, Y., Xiao, B. & Xu, W. (2017). Functional nucleic acids biosensors for living or dead bacteria detection. *Journal of Food Microbiology 1*, 7-13.

Zheng, G., Patolsky, F., Cui, F., Wang, W.U. & Lieber C.M. (2005). Multiplexed electrical detection of cancer markers with nanowire sensor arrays. *Nature Biotechnology 23*, 1294-1301.